HHS Public Access

Author manuscript

Nat Cell Biol. Author manuscript; available in PMC 2015 September 01.

Published in final edited form as:

Nat Cell Biol. 2015 March ; 17(3): 262–275. doi:10.1038/ncb3101.

Huntingtin Functions as a Scaffold for Selective Macroautophagy

Yan-Ning Rui[1,11], **Zhen Xu**[1,11], **Bindi Patel**[8,11], **Zhihua Chen**[1], **Dongsheng Chen**[1], **Antonio Tito**[1,3], **Gabriela David**[6], **Yamin Sun**[1], **Erin F. Stimming**[4], **Hugo Bellen**[5,6,7], **Ana Maria Cuervo**[8,9,10,12], and **Sheng Zhang**[1,2,3,12]

[1]The Brown Foundation Institute of Molecular Medicine, The University of Texas Graduate School of Biomedical Sciences, The University of Texas Medical School at Houston, The University of Texas Health Science Center at Houston (UTHEALTH), 1825 Pressler Street, Houston, TX, 77030

[2]Department of Neurobiology and Anatomy, The University of Texas Graduate School of Biomedical Sciences, The University of Texas Medical School at Houston, The University of Texas Health Science Center at Houston (UTHEALTH), 1825 Pressler Street, Houston, TX, 77030

[3]Programs in Human and Molecular Genetics and Neuroscience, The University of Texas Graduate School of Biomedical Sciences, The University of Texas Medical School at Houston, The University of Texas Health Science Center at Houston (UTHEALTH), 1825 Pressler Street, Houston, TX, 77030

[4]Department of Neurology, The University of Texas Graduate School of Biomedical Sciences, The University of Texas Medical School at Houston, The University of Texas Health Science Center at Houston (UTHEALTH), 1825 Pressler Street, Houston, TX, 77030

[5]Howard Hughes Medical Institute, Baylor College of Medicine, Jan and Dan Duncan Neurological Research Institute, 1250 Moursund Street, Houston, TX 77030

[6]Program in Developmental Biology, Baylor College of Medicine, Jan and Dan Duncan Neurological Research Institute, 1250 Moursund Street, Houston, TX 77030

[12]Corresponding authors: sheng.zhang@uth.tmc.edu. ana-maria.cuervo@einstein.yu.edu.
[11]Equal contributions

Author Contributions

YNR and ZX designed and performed the majority of *Drosophila* studies and most of the studies on starvation- and MG132-induced autophagy response and Tau-ΔC degradation in mammalian cells; BP designed and performed part of the studies on autophagic flux in mammalian cells, and most of the studies of lipophagy and mitophagy, some of the co-IP studies and all the electron microscopy studies and morphometric analysis; ZC, DC, AT and YS contributed to part of these studies; GD performed larva starvation, lysotracker staining and LC3 reporter assay; GD and HB designed experiments, analyzed data and contributed to part of the writing and revision of the manuscript; AMC coordinated the study, designed experiments, analyzed data and contributed to the writing and revision of the manuscript. SZ coordinated the study, designed experiments, analyzed data and contributed to the main writing and revision of the manuscript.

Competing Financial Interests

The authors declare no competing financial interests.

[7]Departments of Molecular and Human Genetics and Neuroscience, Baylor College of Medicine, Jan and Dan Duncan Neurological Research Institute, 1250 Moursund Street, Houston, TX 77030

[8]Department of Development and Molecular Biology, Albert Einstein College of Medicine, Bronx, New York 10461

[9]Department of Anatomy and Structural Biology, Albert Einstein College of Medicine, Bronx, New York 10461

[10]Institute for Aging Studies, Albert Einstein College of Medicine, Bronx, New York 10461

Abstract

Selective macroautophagy is an important protective mechanism against diverse cellular stresses. In contrast to the well-characterized starvation-induced autophagy, the regulation of selective autophagy is largely unknown. Here, we demonstrate that Huntingtin, the Huntington's disease gene product, functions as a scaffold protein for selective macroautophagy but it is dispensable for nonselective macroautophagy. In *Drosophila*, Huntingtin genetically interacts with autophagy pathway components. In mammalian cells, Huntingtin physically interacts with the autophagy cargo receptor p62 to facilitate its association with the integral autophagosome component LC3 and with lysine-63-linked ubiquitin-modified substrates. Maximal activation of selective autophagy during stress is attained by the ability of Huntingtin to bind ULK1, a kinase that initiates autophagy, which releases ULK1 from negative regulation via mTOR. Our data uncover an important physiological function of Huntingtin and provide a missing link in the activation of selective macroautophagy in metazoans.

Introduction

In macroautophagy (hereafter referred to as autophagy), the material to be degraded (cargo) is first sequestered into a double membrane vesicle (autophagosome) that subsequently fuses with the lysosome[1]. Contrary to the "in bulk" engulfment of cytosolic material observed upon induction of autophagy by starvation[1], most nutrient-independent stresses (i.e. proteotoxicity, lipotoxicy, organelle damage) activate selective autophagy in which only the altered cytosolic components are recognized by cargo adaptors such as p62/SQSTM1[2], and then targeted for lysosomal degradation[3, 4]. Despite a growing appreciation of the role of selective autophagy in intracellular quality control and cellular stress response, its regulation and how the autophagy machinery is recruited to the cargo for autophagosome formation are not well-defined. In yeast, scaffold proteins such as Atg11 facilitate the effective recruitment of cargos into autophagosome through their interaction with cargo receptors[5]. However, few such scaffolds have been identified in mammals[6]. A second difference between starvation-induced "in bulk" autophagy and selective autophagy is their regulation. Activation of autophagy upon starvation is attained through repression of the master nutrient sensor mTOR complex 1 (mTORC1), which promotes release and activation of an autophagy initiation kinase ULK1. In contrast, selective autophagy can be activated independently of mTORC1 through relatively poorly understood mechanisms.

Huntingtin (Htt), the gene mutated in Huntington's disease (HD), encodes a large protein with many proposed functions[7–11]. We previously reported defective autophagy in HD affected neurons manifested by the presence of "empty autophagosomes" and suggestive of failure of cargo sequestration[12]. Here, we show that Htt positively modulates selective autophagy but not starvation-induced autophagy in fly and mammalian cells. Htt contributes to cargo recognition by facilitating binding of p62 to ubiquitin (Ub)-K63 modified cargos and to LC3, an integral autophagosome component. In addition, non-overlapping interaction of Htt with ULK1 promotes its activation by dissociation from the mTOR-ULK1 complex and subsequent initiation of selective autophagy. These data support a dual function of Htt as a scaffold in selective autophagy by promoting cargo recognition and autophagy initiation.

Results

Drosophila huntingtin genetically interacts with autophagy pathway components

Homozygous flies lacking its single *htt* homolog ($dhtt^{ko}$) are fully viable with only mild phenotypes[13]. In a genetic screen for Htt's physiological function, ectopic expression of a truncated form of microtubule-binding protein Tau (Tau-ΔC; truncated after V^{382}) induced a prominent collapse of the thorax in $dhtt^{ko}$ flies due to severe underneath muscle loss (Fig. 1a7) not observed by Tau expression alone, and accelerated decline in mobility and life-span. These phenotypes were fully rescued by the *dhtt* genomic rescue transgene ("$dhtt^{Rescue}$")[13] (Fig. 1a and Supplementary Figure 1a–c), suggesting that *dhtt* protects against Tau-induced pathogenic effects.

Although heterozygous $dhtt^{ko}$/+ flies expressing Tau (ATau; $dhtt^{ko}$/+) appear normal, removing in these flies of a single copy of the fly LC3 gene, *atg8a* ($atg8a^{d4}$ mutant)[14] also induced collapsed thorax and muscle loss, which could be phenocopied by expressing Tau in homozygous $atg8a^{d4-/-}$ flies alone (Fig. 1b and Supplementary Figure 1d). Four additional components of the early steps of the autophagy pathway, *atg1* (ULK1), *atg7* and *atg13,* and an adaptor for the selective recognition of autophagic cargo, *Ref(2)P* (p62)[15], also exhibit strong genetic interactions with *dhtt* (Fig. 1c and Supplementary Figure 1e). Consistent with its pivotal role in autophagy initiation[1], loss of *atg1* induced the strongest defect and Tau expression could induce a mild muscle loss phenotype even in heterozygous null $atg1^{\Delta 3d}$ (Fig. 1c). Collectively, these genetic interaction studies suggest a role of *dhtt* in autophagy.

Drosophila huntingtin positively regulates autophagy *in vivo*

Using the mCherry-GFP-Atg8a fusion reporter to directly measure autophagic flux in adult $dhtt^{ko-/-}$ brains[16], we found similar number of red fluorescent punctae (acidic autolysosomes originating from autophagosome/lysosome fusion) in young mutant and control flies, but the number of punctae was reduced in old $dhtt^{ko-/-}$ brains when compared to age-matched controls (Fig. 1d,e). Since we did not observe autophagosome accumulation (colocalized green and red puncta), we concluded that absence of *dhtt* in older animals is associated with reduced autophagosome formation. The fact that levels of Ref(2)P were significantly higher in old $dhtt^{ko-/-}$ brains compared to brains from age-matched wildtype

control (Fig. 1f,g) suggested a possible preferential compromise in selective autophagy in these animals.

Consistent with the role of basal selective autophagy in quality control in non-dividing cells[17], we found that brains from 5 weeks old $dhtt^{ko-/-}$ contained almost double amount of ubiquitinated proteins, marker of quality control failure, than wildtype flies (Supplementary Fig 2a). Since genetic interaction analysis and specific ubiquitin proteasome system (UPS) reporters all failed to reveal a functional link between *dhtt* and the UPS pathway (Supplementary Figure 2b–f), we propose that the defects in autophagic activity are the main cause of diminished quality control and increased accumulation of ubiquitinated proteins in $dhtt^{ko-/-}$ mutants.

Drosophila huntingtin is required for intracellular quality control

Selective autophagy is induced in response to proteotoxic stress. The truncated Tau-ΔC used in our genetic studies, is preferentially degraded through autophagy in cortical neurons[18], serving as a model of proteotoxicity when ectopically expressed. We confirmed lower stability of Tau-ΔC compared to full-length Tau in wildtype flies (Supplementary Figure 3a) and in UPS mutants, but found significantly higher levels of Tau-ΔC when expressed in *atg8a* and in $dhtt^{ko-/-}$ mutant flies (Fig. 1h–j), suggesting that autophagy is essential for the clearance of Tau-ΔC also in flies and that *dhtt* plays a role in this clearance.

In contrast, loss of *dhtt* did not affect flies' adaptation to nutrient deprivation, which typically induces robust "in bulk" autophagy[19]. Fat bodies of early third instar larvae expressing mCherry-Atg8, where starvation-induced autophagy can be readily detected[20], failed to reveal any significant difference between wildtype and $dhtt^{ko-/-}$ flies and they die at the same rate as wildtype flies when tested for starvation resistance (Supplementary Figure 2g–i). Thus, although *dhtt* is necessary for selective autophagy of toxic proteins such as Tau-ΔC, it is dispensable for starvation-induced autophagy in flies.

Huntingtin's function is conserved from flies to humans

Expression of human Htt (hHtt) in $dhtt^{ko-/-}$ null rescued both the mobility and longevity defects of $dhtt^{ko-/-}$ mutants and partially rescued the Tau-induced morphological and behavioral defects of $dhtt^{ko-/-}$ flies (Fig. 2a and Supplementary Figure 3b–f). hHtt also suppressed almost all the autophagic defects observed in $dhtt^{ko-/-}$, including decreased levels of autolysosomes, increased levels of Ref(2)P and of total ubiquitinated proteins, and accumulation of ectopically expressed Tau-ΔC (Fig. 2b–e and Supplementary Figure 3g–i), suggesting that the involvement of *dhtt* in autophagy is functionally conserved. In fact, confluent mouse fibroblasts knocked down for Htt (Htt(−)) displayed significantly lower basal rates of long-lived proteins' degradation than control cells, which were no longer evident upon chemical inhibition of lysosomal proteolysis or of macroautophagy, thus confirming an autophagic origin of the proteolytic defect (Fig. 2g,h). Htt(−) fibroblasts also displayed higher p62 levels and accumulate ubiquitin aggregates even in absence of a proteotoxic challenge (Fig. 2i,j). Similar to $dhtt^{ko-/-}$ flies, Htt knockdown in mammalian cells did not affect degradation of CL1-GFP (a UPS reporter), β-catenin (a UPS canonical substrate) or proteasome peptidase activities (Supplementary Figure 4a–c). Reduced

autophagic degradation in Htt(−) cells was not due to a primary lysosomal defect, as depletion of Htt did not reduce lysosomal acidification, endo-lysosomal number (if anything, we observed an expansion of this compartment) or other lysosomal functions such as endocytosis (transferrin internalization) (Supplementary Figure 4d–h). In fact, analysis of the lysosomal degradation of LC3-II revealed that autophagic flux and autophagosome formation were preserved and even enhanced in Htt(−) fibroblasts at basal conditions (Fig. 2k,l).

We have previously shown a similar apparent dichotomy - reduced autophagic degradation of cargo (long-lived proteins and p62) with normal or increased formation and clearance of LC3 positive autophagic vesicles - in cells from HD patients[12]. Since in this pathological setting, we observed an "empty autophagosome" phenotype resulting from defective cargo sequestration, we performed electron microscopy (EM). We found that the overall size and number of the autophagic/lysosomal compartments was expanded in Htt(−) fibroblasts under basal conditions but that, contrary to the organelles and electron-dense cargo noticeable in the vacuoles in the control cells, a larger fraction of the vesicular structures in Htt(−) fibroblasts lacked visible content or had a mixed cargo composition reflective of "in bulk" autophagy (Fig. 2m,n). Immunogold staining for LC3 confirmed the autophagic nature of the Htt(−) cells' empty vesicles (Fig. 2o). Thus, similar to flies, Htt is also required for effective autophagy in mammals and its depletion affects the autophagic process early at the step of selective cargo recognition.

Mammalian Huntingtin is required for selective autophagy

In light of the above observed role of Htt in autophagy under basal conditions, we then analyzed the requirement for Htt in autophagy activated in response to different cellular stressors, when only specific cytosolic cargo is degraded. The reduced rates of autophagic degradation of long-lived proteins observed in Htt(−) fibroblasts, become even more pronounced upon exposure to proteotoxic stress (inhibition of proteasome degradation), lipotoxic stress (oleic challenge) or the mitochondrial depolarizing agent FCCP (Fig. 3a). However, upon starvation (serum removal or incubation in nutrient-free media), control and Htt(−) fibroblasts displayed a similar increase in long lived proteins' degradation and in fragmentation of GST-BHMT, a cargo-based end-point assay for autophagy[21] (Fig. 3a,b). In contrast, accumulation of fragmented GST-BHMT was almost abolished in Htt(−) fibroblasts subjected to proteotoxic stress by proteasome inhibition (Fig. 3c).

To further analyze the involvement of Htt in selective autophagy, we directly tracked the cargo targeted in each of these stress conditions. In stably-transfected HeLa cells with inducible expression of Tau-ΔC, degradation of Tau-ΔC was mostly dependent on autophagy (sensitive to 3-methyladenine or Atg7 knockdown but insensitive to proteasome inhibition) (Supplementary Figure 4i–k). Htt knockdown dramatically blocked Tau-ΔC turnover (Fig. 3d,e), indicating that, similar to flies, Htt is required for the autophagy-mediated degradation of Tau-ΔC.

We next induced selective degradation of lipid droplets (lipophagy) by cell loading with oleic acid[22, 23]. Htt(−) fibroblasts displayed higher sensitivity to lipid challenges and a more pronounced accumulation of lipid droplets (Fig. 3f–h). Lipid accumulation in Htt(−)

fibroblasts was mostly due to their reduced ability to mobilize and break down intracellular lipid stores, as they failed to increase mitochondrial respiration in response to the lipogenic challenge and displayed lower rates of lipid beta-oxidation (Fig. 3i, j). Immunostaining revealed significantly lower colocalization of LC3 with Bodipy-labeled lipid droplets in Htt(−) cells (Fig. 3k,l), further supporting that Htt is required for selective lipophagy. Similarly, Htt(−) fibroblasts showed a comparatively higher content of depolarized mitochondria (labeled with MitoTracker® but negative for MitoTracker® Red CMXRos staining) and reduced colocalization between LC3 and MitoTracker®-highlighted mitochondria than control cells, in support of reduced mitophagy (Fig. 3m–p).

Ultrastructural analysis of control and Htt(−)cells upon exposure to these three different stressors confirmed the fluorescence data (Fig. 4a–c). Thus, the most abundant fraction of autophagosomes in control cells treated with a proteasome inhibitor were those containing aggregate proteinaceous material, whereas in Htt(−) cells most of the observed autophagic vacuoles had a clear lumen and aggregates were instead detectable free in the cytosol (Fig. 4a). Similarly, treatment with oleic acid or FCCP, increased the fraction of autophagic vacuoles containing lipids or mitochondria, respectively, in control cells whereas this switch toward a specific autophagic cargo was not observed in Htt(−) cells (Fig. 4b–c). Interestingly, in contrast to the higher autophagic vacuole content observed in Htt(−) fibroblasts under basal conditions (Fig. 2m,n), number and cell fraction occupied by autophagic vacuoles upon exposure to any of these stressors were significantly lower in Htt(−) than in control cells (Fig. 4a–c), in support of a failure to maximally induced selective autophagy in Htt-deficient cells.

Complete ablation of Htt (mouse embryonic fibroblasts (MEFs) from mice knock-out for Htt[24]) or Htt knockdown in other cell types (neuroblastoma N2a cells and mouse striatal cells), also lead to higher levels of p62 and reduced colocalization of LC3 with markers of lipid droplets or mitochondria upon exposure to oleic acid or FCCP, respectively (Fig. 5). Overall, our results support that Htt is dispensable for starvation-induced autophagy but essential for at least three different types of selective autophagy, aggrephagy of either a specific protein (Tau) or a pool of aggregate proteins (proteasome inhibition), lipophagy and mitophagy.

Further analysis of changes in autophagic flux in absence of Htt in different cell types under different experimental conditions revealed that, in contrast to the increase in basal autophagosome formation and autophagic flux observed in Htt(−) fibroblasts (Fig. 2k,l), Htt depletion in HeLa cells had indiscernible effects on basal LC3-II flux and on GST-BHMT fragmentation under basal conditions (Supplementary Figure 5a,b). These data likely reflect the lower dependence on Htt-mediated selective autophagy in these rapidly dividing cells, where quality control is less important. However, when we forced activation of quality control selective autophagy in these cells by inflicting proteotoxic stress with the proteasome inhibitor, Htt knockdown markedly blocked the induction of autophagy visible in the control cells as an increase in steady-state levels and clearance of LC3-II (Fig. 6a). Immunostaining for LC3 confirmed a reduced increase in the number of LC3-positive puncta in the Htt(−) HeLa cells upon proteotoxic stress (Fig. 6b,c). Transfection with GFP-Htt restored the defective autophagic flux during proteotoxic stress both in Htt(−) HeLa cells

and in Htt-KO MEFs, but did not affect autophagy activation in response to serum removal (Supplementary Figure 5c,d). Blockage of lysosomal proteolysis with bafilomycin-A1 in Htt(−) cells exposed to proteasome inhibition still increased the number of LC3-positive puncta (Fig. 6b,d), suggesting that, in agreement with the EM data (Fig. 4), autophagosome clearance is normal in Htt-depleted cells and that their reduced LC3 flux during proteotoxic stress is mainly due to reduced autophagosome formation. Consistently, double labeling with the lysosome marker LAMP1 revealed lysosomal accumulation of LC3 in bafilomycin-A1 treated cells in both control and Htt(−) cells, indicating that fusion of autophagosomes with lysosomes still occurs in the absence of Htt (Supplementary Figure 5e). In contrast, Htt knockdown did not significantly affect the levels or processing of LC3-II upon induction of nonselective autophagy by nutrient depletion (Supplementary Figure 5f). We found similar defects in induction of selective autophagy upon exposure to proteasome inhibitors, oleic acid or FCCP upon Htt depletion in mouse fibroblasts, MEFs, striatal and neuroblastoma cells expressing the mCherry-GFP-LC3 fusion reporter, whereas their ability to upregulate autophagic flux in response to nutritional deprivation remained unaffected (Supplementary Figure 5g–k). These results support that Htt is important in selective autophagy for both initiation of autophagosome formation and cargo recognition.

Huntingtin physically interacts with p62 and ULK1 proteins

To explore how Htt is involved in autophagy regulation, we next examined potential physical interactions between Htt and the autophagy components identified in our fly-based genetic screens (Fig. 1). Using whole-animal extracts from a genome-tagging fly line expressing 3xHA-tagged dHtt, we found that *dhtt* strongly co-immunoprecipitated with endogenous Ref(2)P (Fig. 6e). Experiments in mammalian cells confirmed co-immunoprecipitation of both, endogenous and tagged Htt and p62, between them and with ULK1, the mammalian Atg1 homolog[25] (Fig. 6f, Supplementary Figure 6a–d). Notably, we previously reported that p62 co-localized and interacted with mutant-Htt in autophagosomes[12]. Hence, results from the fly and mammalian systems together support that p62 and ULK1 are conserved binding partners of Htt.

Intriguingly, the amount of endogenous p62 that co-immunoprecipitated with endogenous Htt was significantly increased upon induction of proteotoxic stress (proteasome inhibitor treatment), whereas the level of co-immunoprecipitated ULK1 remained similar (Fig. 6g). Immunofluorescence for endogenous Htt and p62 in HeLa cells also revealed enrichment of Htt in the large p62-positive bodies (sequestosomes)[26] that form around the nucleus upon proteasome inhibition (Fig. 6h), suggesting a translocation of Htt to the p62 bodies in response to autophagy induction. Tagged-ULK1 has been shown to co-localize with p62[27], raising the possibility that Htt might form a tertiary complex with p62 and ULK1.

To map the regions responsible for Htt's association with p62 and ULK1, we generated Htt deletions and through co-IP identified two non-overlapping conserved regions1[13,28] in Htt, the C-terminal D6 and the middle D3 regions that bind to p62 and ULK1, respectively (Fig. 6i–k and Supplementary Figure 6e–g).

Huntingtin facilitates p62-mediated cargo recognition efficiency

Given the defective sequestration of selective cargo inside autophagosomes in Htt(−) cells and the direct interaction between Htt and p62, we investigated if Htt functions with p62 in cargo recognition. p62 is involved in selective autophagy by simultaneous binding with LC3 and ubiquitinated cargos for their subsequent engulfment by the forming autophagic membrane[2]. Cargo recognition by p62 initiates with the formation of sequestosomes (detergent resistant p62 bodies)[2, 26]. Accordingly, treatment with proteasome inhibitors gradually decreases soluble p62 and increased insoluble p62 in control cells. However, p62 redistribution and formation of large p62 bodies were no longer observed upon depletion of Htt (Fig. 7a–c and Supplementary Figure 7a–c; depletion of Beclin 1, essential for autophagosome formation[1,25] is shown as positive control). In contrast, the fraction of cellular p62 degraded by autophagy during starvation did not change upon Htt knockdown (Supplementary Figure 7d).

Three functional domains in p62 coordinate its roles in selective autophagy: the self-polymerization (PB1) and ubiquitin-binding (UBA) domains are critical for p62 body formation[2], and the middle motif (LIR) for its interaction with LC3 for cargo-based autophagic degradation[29]. We found that knockdown of Htt had no obvious effect on p62 polymerization (HA-p62 and Myc-p62 interaction) or its interaction with ubiquitinated proteins containing the K48 linkage-specific modification (Ub-K48), but strikingly reduced the amount of p62 that co-immunoprecipitated with ubiquitinated substrates containing the K63 linkage-specific modification[30] (Ub-K63) (Supplementary Figure 7e–g). These findings were also reproduced using transfected HA-tagged Ub-K63 and Ub-K48 and pull downs with anti-HA (to discard non-specific antibody effects) (Supplementary Figure 7h–i) and in Htt-KO MEFs (to discard non-specific siRNA-mediated effects) (Fig. 7d–e). The above results raise the possibility that Tau-ΔC is also a target of Ub-K63 modification. Indeed, we found that Tau-ΔC protein was preferentially modified by Ub-K63 but not Ub-K48 in the inducible HeLa cells (Fig. 7f). Co-immunoprecipitation experiments showed that p62 physically interacts with Tau-ΔC and their affinity was compromised after Htt knockdown (Fig. 7g). Overall these findings indicate that Htt facilitates p62 binding to Ub-K63-modified proteins that are preferentially degraded by selective autophagy[31].

Lastly, we investigated the effect of Htt knockdown in the interaction of p62 with LC3. The ability of LC3 to co-immunoprecipitate endogenous p62 was markedly reduced in Htt(−) cells and, accordingly, colocalization of p62 and LC3 was also significantly reduced upon Htt loss (Fig. 7h–j). Although it is not possible to discriminate if the reduced p62 and LC3 interaction is primarily due to the loss of Htt or secondary to the inability of p62 to bind K63 ubiquitinated cargo, these findings uncover an essential role for Htt in p62-dependent cargo recognition required for proper sequestration of specific cargo into autophagosomes during selective autophagy.

Huntingtin/ULK1 and mTOR/ULK1 complexes are mutually exclusive

To investigate the basis for the observed defective autophagosome biogenesis in Htt(−) cells in response to different stressors, we followed up on the physical (Fig. 6f) and genetic (Fig. 1c) interaction of Htt with ULK1, the kinase essential for initiation of both selective and

nonselective autophagy[25]. In control cells, both starvation and proteotoxicity (proteasome inhibition) significantly boosted ULK1 kinase activity, measured as increased phosphorylation of MBP, a pseudo-substrate for ULK1[25], but Htt knockdown only attenuated proteasome inhibition-mediated ULK1 activation (Fig. 8a). These results suggest that Htt could contribute to regulate initiation of selective autophagy by modulating ULK1 activation while not affecting starvation induced nonselective autophagy. Consistent with this hypothesis, Htt has no significant impact on AMPK which positively regulates ULK1 kinase activity in response to energy depletion, presumably by interacting and phosphorylating ULK1[32–34]. Htt knockdown did not disrupt the interaction between AMPK and ULK1, nor interfered with AMPK-mediated ULK1 phosphorylation at Ser555 (Supplementary Figure 8a,b), two mechanisms of regulation that are critical for AMPK-induced ULK1 activation[35].

To determine how Htt specifically activates selective autophagy but not nonselective autophagy when they both share common regulators including ULK1, we systematically examined several established mechanisms governing ULK1 kinase activity. Maximal activation of ULK1 is attained by forming a stable quaternary complex with FIP200, Atg13 and Atg101[25]. Pull-down assays revealed that Htt did not affect the stability of this complex (Supplementary Figure 8c). ULK1 is also regulated by the central nutrient sensor mTORC1, which binds to ULK1 and represses its kinase activity to prevent autophagy initiation. Inactivation of mTORC1 during starvation triggers release of active ULK1 from this complex and initiation of nonselective autophagy[36], whereas the mechanisms that counterbalance the inhibitory effect of mTORC1 on ULK1 for activation of selective autophagy remain poorly understood. We first tested whether Htt affected the kinase activity of mTOR and consequently its inhibitory effect on ULK1. Neither Htt knockdown nor Htt overexpression showed any obvious effect on mTOR kinase activity when assessed by the phosphorylation of the downstream mTOR effector S6K at Thr389[36] under basal conditions or upon activation of mTOR by the upstream regulator Rheb (Supplementary Figure 8d,e). This result was further confirmed by an *in vitro* kinase assay using GST-4E-BP1, a substrate readily phosphorylated by mTOR at Ser65 after mTOR activation. Ser65-GST-4E-BP1 phosphorylation was unaffected by Htt knockdown (Supplementary Figure 8f). Thus, Htt might not activate ULK1 by directly inhibiting mTOR activity.

Excitingly, although ULK1 co-immunoprecipitated with Htt, mTOR, and Raptor, an adaptor protein critical for mTORC1 activity (Fig. 8b), Htt/ULK1 and mTOR/Raptor/ULK1 exist as two separate mutually exclusive complexes. Specifically, co-immunoprecipitation assays showed that Htt could pull-down ULK1 but not mTOR or Raptor (Fig. 8c), and both mTOR and Raptor co-immunoprecipitated ULK1 but not Htt (Fig. 8d). Similar physical interactions were observed for endogenous Htt, ULK1 and mTOR proteins in MEFs (Fig. 8e,f; Htt-KO and ULK1-KO[37] as controls) and neuroblastoma N2a cells (Supplementary Figure 8g–i), thus confirming the existence of two mutually exclusive ULK1/Htt and ULK1/mTOR complexes. This mutual exclusion indicates that Htt may promote ULK1 activation during selective autophagy by directly competing for the inhibitory binding of mTORC1 to ULK1. Indeed, under all three different stress conditions, we observed an increased interaction between ULK1 and Htt at the expense of mTOR, while Htt depletion largely abolished this

competitive effect (Fig. 8g and Supplementary Figures 8j,k). Consistently, overexpression of Htt significantly blocked mTOR-mediated repression of ULK1. Basal ULK1-dependent phosphorylation of MBP can be detected in the kinase assay under rich nutritional conditions but not with the kinase-dead ULK1 mutant (FLAG-ULK1-KD) (Fig. 8a). This basal ULK1 activity is sensitive to regulation by mTOR, as overexpression of Myc-mTOR substantially repressed MBP phosphorylation and overexpression of a kinase-dead Myc-mTOR mutant showed the opposite effect, probably through a dominant-negative mechanism (Fig. 8h). Interestingly, overexpression of Htt significantly relieved this mTOR-mediated repression of basal ULK1 kinase activity (Fig. 8h), suggesting that Htt antagonizes the negative regulation of mTOR on ULK1 and promotes activation of selective autophagy even in the presence of active mTOR (rich media) by directly competing away ULK1 from the mTORC1/ULK1 complex. Indeed, co-immunoprecipitation assays revealed that Htt overexpression dramatically reduced the amount of endogenous mTOR and Raptor proteins associated with ULK1 (Fig. 8i), providing further support for this competition model. Changes in Htt protein levels may also contribute to modulate Htt function on autophagy under physiological conditions, since after exposure to stressors that induce selective autophagy but not in response to starvation, we found modest elevations of endogenous Htt levels in fibroblasts and neuroblastoma N2a cells (Supplementary Figure 8l,m).

Discussion

Selective autophagy is important for intracellular quality control and the cellular stress response but its regulation and how the autophagy machinery is recruited to the cargo for autophagosome formation are still poorly-defined processes. In this work, we show that Htt is a scaffold protein that promotes selective autophagy through its ability to simultaneously interact with components involved in two major autophagy steps, p62 and ULK1, and thus modulate both cargo recognition efficiency and autophagosome initiation. First, Htt releases the inhibitory effect of mTOR over ULK1, by directly competing away this kinase from the mTORC1 complex. Second, binding of Htt to p62 enhances the association between this cargo receptor and its Ub-K63-modified substrates. We propose a scaffolding role for Htt in selective autophagy whereby the ability of Htt to simultaneously bind ULK1 and p62 assures the spatial proximity between cargo recognition and autophagy initiation components (Fig. 8j).

We found that Htt is required for at least three types of selective autophagy (aggregophagy, lipophagy and mitophagy) but is dispensable for starvation-induced autophagy. Selective recognition of cargo requires receptors including p62, and Htt facilitates p62-mediated cargo recognition, at least in part, by enhancing the affinity between p62 and Ub-K63-modified cargos[38] and LC3. Selective formation of an autophagosome around the p62-recognized cargo has been attributed to the ability of p62 to simultaneously bind cargo and LC3. However, autophagy initiation requires events that precede lipid conjugation of LC3, such as recruitment to the sites of autophagosome formation of ULK1, one of the earliest autophagy effectors. We propose that Htt directs ULK1 to these sites by forming an Htt/ULK1 complex distinct from the mTOR/ULK1 complex. Of note, both Htt and mTOR contain HEAT repeats[39], which could be the basis of their mutually exclusive interaction with ULK1 and of the Htt's ability to compete UKL1/mTOR binding for maximal activation of selective

autophagy. Under basal conditions, binding of Htt to the pool of constitutively active ULK1 identified in this study might be sufficient for preserving basal autophagy-dependent intracellular quality control, potentially by competing and shielding ULK1 from the inhibitory mTORC1 complex. Although how this competing activity of Htt is repressed under basal conditions requires future investigation, it is possible that changes in Htt levels, subcellular location or its myriad of posttranslational modifications[40–47] could contribute to regulate Htt's function to fine-tune the proper cellular autophagic response against a variety of cellular stresses.

Noticeably, animals deficient for Htt, ULK1 and p62 show distinctive phenotypes. Htt KO mice die at embryonic day E7.5[48–50], whereas p62 and ULK1-KO are viable[37, 51–54]. These differences are likely partially due to the additional roles each protein plays besides autophagy. For example, the earlier lethality of the Htt-KO has been primarily attributed to Htt's essential role in extraembryonic tissues[55, 56]. Furthermore, only one Htt gene exists in both the fly and most vertebrate genomes, whereas ULK1 and ULK2 seem capable to compensate from each other[37, 53, 54, 57] and the function of p62 in autophagic cargo recognition shows some redundancy with other receptors such as NBR1. Interestingly, p62-KO mice display adult onset neurodegeneration with elevated level of K63-ubiquitinated Tau in the brain[58, 59], reminiscent of the brain degeneration observed upon reduced Htt expression or Htt postnatal deletion[60, 61].

Connections of Htt with autophagy have previously been described[11, 42, 62–64] and we also reported autophagy abnormalities ("empty autophagosomes" phenotype) in the context of HD[12]. Since deleting polyQ tract in Htt enhances neuronal autophagic activity and longevity in mice[65], it is attractive to propose that polyQ expansion compromises Htt's role in selective autophagy.

Supplementary Material

Refer to Web version on PubMed Central for supplementary material.

Acknowledgments

We are grateful to Dr. Thomas Neufeld and Dr. Udai Pandey for their fly lines; Dr. Patrick B. Dennis for the pRK5-GST-BHMT plasmid; Dr. Didier Contamine for anti-Ref(2)P antibody; Dr. Bezprozvanny for MEF-Htt-WT and MEF-Htt-KO lines; Dr. Kundu for MEF-ULK1-KO and MEF-ULK1-WT lines; Dr. Juan Botas for UAS-hHtt DNA and fly lines. We also thank Dr. Zhenmei Mao for technical assistance in confocal microscope, Dr. Zhaoxia Sun and Dr. Norbert Perrimon for critically reading the manuscript. HJB is an investigator of the HHMI and supported by the R&R Belfer and Hufftington foundations. Gabriela David was supported by a T32 developmental biology training grant from the NICHD. This work was supported by NIH grants R01-NS069880 (to S.Z.) and P01-AG031782 and AG038072 (to A.M.C.) and the generous support of R&R Belfer (to A.M.C.).

References

1. He C, Klionsky DJ. Regulation mechanisms and signaling pathways of autophagy. Annual review of genetics. 2009; 43:67–93.
2. Bjorkoy G, Lamark T, Johansen T. p62/SQSTM1: a missing link between protein aggregates and the autophagy machinery. Autophagy. 2006; 2:138–139. [PubMed: 16874037]
3. Johansen T, Lamark T. Selective autophagy mediated by autophagic adapter proteins. Autophagy. 2011; 7:279–296. [PubMed: 21189453]

4. Lamark T, Johansen T. Aggrephagy: selective disposal of protein aggregates by macroautophagy. Int J Cell Biol. 2012; 2012:736905. [PubMed: 22518139]
5. Lynch-Day MA, Klionsky DJ. The Cvt pathway as a model for selective autophagy. FEBS Lett. 2010; 584:1359–1366. [PubMed: 20146925]
6. Jin M, Liu X, Klionsky DJ. SnapShot: Selective Autophagy. Cell. 2013; 152:368–368. e362. [PubMed: 23332767]
7. The Huntington's Disease Collaborative Research Group. A novel gene containing a trinucleotide repeat that is expanded and unstable on Huntington's disease chromosomes. Cell. 1993; 72:971–983. [PubMed: 8458085]
8. Cattaneo E, Zuccato C, Tartari M. Normal huntingtin function: an alternative approach to Huntington's disease. Nat Rev Neurosci. 2005; 6:919–930. [PubMed: 16288298]
9. Caviston JP, Holzbaur EL. Huntingtin as an essential integrator of intracellular vesicular trafficking. Trends Cell Biol. 2009; 19:147–155. [PubMed: 19269181]
10. Harjes P, Wanker EE. The hunt for huntingtin function: interaction partners tell many different stories. Trends in biochemical sciences. 2003; 28:425–433. [PubMed: 12932731]
11. Martin DD, Ladha S, Ehrnhoefer DE, Hayden MR. Autophagy in Huntington disease and huntingtin in autophagy. Trends in neurosciences. 2014
12. Martinez-Vicente M, et al. Cargo recognition failure is responsible for inefficient autophagy in Huntington's disease. Nat Neurosci. 2010; 13:567–576. [PubMed: 20383138]
13. Zhang S, Feany MB, Saraswati S, Littleton JT, Perrimon N. Inactivation of Drosophila Huntingtin affects long-term adult functioning and the pathogenesis of a Huntington's disease model. Dis Model Mech. 2009; 2:247–266. [PubMed: 19380309]
14. Pircs K, et al. Advantages and limitations of different p62-based assays for estimating autophagic activity in Drosophila. PloS one. 2012; 7:e44214. [PubMed: 22952930]
15. Bartlett BJ, et al. p62, Ref(2)P and ubiquitinated proteins are conserved markers of neuronal aging, aggregate formation and progressive autophagic defects. Autophagy. 2011; 7:572–583. [PubMed: 21325881]
16. Nezis IP, et al. Autophagic degradation of dBruce controls DNA fragmentation in nurse cells during late Drosophila melanogaster oogenesis. J Cell Biol. 2010; 190:523–531. [PubMed: 20713604]
17. Rubinsztein DC. The roles of intracellular protein-degradation pathways in neurodegeneration. Nature. 2006; 443:780–786. [PubMed: 17051204]
18. Dolan PJ, Johnson GV. A caspase cleaved form of tau is preferentially degraded through the autophagy pathway. J Biol Chem. 2010; 285:21978–21987. [PubMed: 20466727]
19. Mortimore GE, Poso AR. Intracellular protein catabolism and its control during nutrient deprivation and supply. Annu Rev Nutr. 1987; 7:539–564. [PubMed: 3300746]
20. Mauvezin C, Ayala C, Braden CR, Kim J, Neufeld TP. Assays to monitor autophagy in Drosophila. Methods. 2014; 68:134–139. [PubMed: 24667416]
21. Dennis PB, Mercer CA. The GST-BHMT assay and related assays for autophagy. Methods Enzymol. 2009; 452:97–118. [PubMed: 19200878]
22. Singh R, et al. Autophagy regulates lipid metabolism. Nature. 2009; 458:1131–1135. [PubMed: 19339967]
23. Koga H, Kaushik S, Cuervo AM. Altered lipid content inhibits autophagic vesicular fusion. FASEB J. 2010; 24:3052–3065. [PubMed: 20375270]
24. Zhang H, et al. Elucidating a normal function of huntingtin by functional and microarray analysis of huntingtin-null mouse embryonic fibroblasts. BMC Neurosci. 2008; 9:38. [PubMed: 18412970]
25. Ganley IG, et al. ULK1.ATG13.FIP200 complex mediates mTOR signaling and is essential for autophagy. J Biol Chem. 2009; 284:12297–12305. [PubMed: 19258318]
26. Bjorkoy G, et al. p62/SQSTM1 forms protein aggregates degraded by autophagy and has a protective effect on huntingtin-induced cell death. J Cell Biol. 2005; 171:603–614. [PubMed: 16286508]
27. Itakura E, Mizushima N. p62 Targeting to the autophagosome formation site requires self-oligomerization but not LC3 binding. J Cell Biol. 2011; 192:17–27. [PubMed: 21220506]

28. Li Z, Karlovich CA, Fish MP, Scott MP, Myers RM. A putative Drosophila homolog of the Huntington's disease gene. Hum Mol Genet. 1999; 8:1807–1815. [PubMed: 10441347]
29. Pankiv S, et al. p62/SQSTM1 binds directly to Atg8/LC3 to facilitate degradation of ubiquitinated protein aggregates by autophagy. J Biol Chem. 2007; 282:24131–24145. [PubMed: 17580304]
30. Newton K, et al. Ubiquitin chain editing revealed by polyubiquitin linkage-specific antibodies. Cell. 2008; 134:668–678. [PubMed: 18724939]
31. Kirkin V, McEwan DG, Novak I, Dikic I. A role for ubiquitin in selective autophagy. Mol Cell. 2009; 34:259–269. [PubMed: 19450525]
32. Egan DF, et al. Phosphorylation of ULK1 (hATG1) by AMP-activated protein kinase connects energy sensing to mitophagy. Science. 2011; 331:456–461. [PubMed: 21205641]
33. Kim J, Kundu M, Viollet B, Guan KL. AMPK and mTOR regulate autophagy through direct phosphorylation of Ulk1. Nat Cell Biol. 2011; 13:132–141. [PubMed: 21258367]
34. Shang L, et al. Nutrient starvation elicits an acute autophagic response mediated by Ulk1 dephosphorylation and its subsequent dissociation from AMPK. Proc Natl Acad Sci U S A. 2011; 108:4788–4793. [PubMed: 21383122]
35. Alers S, Loffler AS, Wesselborg S, Stork B. Role of AMPK-mTOR-Ulk1/2 in the regulation of autophagy: cross talk, shortcuts, and feedbacks. Mol Cell Biol. 2012; 32:2–11. [PubMed: 22025673]
36. Laplante M, Sabatini DM. mTOR signaling in growth control and disease. Cell. 2012; 149:274–293. [PubMed: 22500797]
37. Kundu M, et al. Ulk1 plays a critical role in the autophagic clearance of mitochondria and ribosomes during reticulocyte maturation. Blood. 2008; 112:1493–1502. [PubMed: 18539900]
38. Seibenhener ML, et al. Sequestosome 1/p62 is a polyubiquitin chain binding protein involved in ubiquitin proteasome degradation. Mol Cell Biol. 2004; 24:8055–8068. [PubMed: 15340068]
39. Andrade MA, Bork P. HEAT repeats in the Huntington's disease protein. Nat Genet. 1995; 11:115–116. [PubMed: 7550332]
40. Ehrnhoefer DE, Sutton L, Hayden MR. Small changes, big impact: posttranslational modifications and function of huntingtin in Huntington disease. The Neuroscientist: a review journal bringing neurobiology, neurology and psychiatry. 2011; 17:475–492.
41. Jeong H, et al. Acetylation targets mutant huntingtin to autophagosomes for degradation. Cell. 2009; 137:60–72. [PubMed: 19345187]
42. Martin DD, et al. Identification of a post-translationally myristoylated autophagy-inducing domain released by caspase cleavage of huntingtin. Hum Mol Genet. 2014; 23:3166–3179. [PubMed: 24459296]
43. Schilling B, et al. Huntingtin phosphorylation sites mapped by mass spectrometry. Modulation of cleavage and toxicity. J Biol Chem. 2006; 281:23686–23697. [PubMed: 16782707]
44. Steffan JS, et al. SUMO modification of Huntingtin and Huntington's disease pathology. Science. 2004; 304:100–104. [PubMed: 15064418]
45. Wellington CL, Hayden MR. Caspases and neurodegeneration: on the cutting edge of new therapeutic approaches. Clin Genet. 2000; 57:1–10. [PubMed: 10733228]
46. Wellington CL, et al. Inhibiting caspase cleavage of huntingtin reduces toxicity and aggregate formation in neuronal and nonneuronal cells. J Biol Chem. 2000; 275:19831–19838. [PubMed: 10770929]
47. Yanai A, et al. Palmitoylation of huntingtin by HIP14 is essential for its trafficking and function. Nat Neurosci. 2006; 9:824–831. [PubMed: 16699508]
48. Duyao MP, et al. Inactivation of the mouse Huntington's disease gene homolog Hdh. Science. 1995; 269:407–410. [PubMed: 7618107]
49. Nasir J, et al. Targeted disruption of the Huntington's disease gene results in embryonic lethality and behavioral and morphological changes in heterozygotes. Cell. 1995; 81:811–823. [PubMed: 7774020]
50. Zeitlin S, Liu JP, Chapman DL, Papaioannou VE, Efstratiadis A. Increased apoptosis and early embryonic lethality in mice nullizygous for the Huntington's disease gene homologue. Nat Genet. 1995; 11:155–163. [PubMed: 7550343]

51. Duran A, et al. The atypical PKC-interacting protein p62 is an important mediator of RANK-activated osteoclastogenesis. Developmental cell. 2004; 6:303–309. [PubMed: 14960283]
52. Rodriguez A, et al. Mature-onset obesity and insulin resistance in mice deficient in the signaling adapter p62. Cell metabolism. 2006; 3:211–222. [PubMed: 16517408]
53. Cheong H, Lindsten T, Wu J, Lu C, Thompson CB. Ammonia-induced autophagy is independent of ULK1/ULK2 kinases. Proc Natl Acad Sci U S A. 2011; 108:11121–11126. [PubMed: 21690395]
54. Lee EJ, Tournier C. The requirement of uncoordinated 51-like kinase 1 (ULK1) and ULK2 in the regulation of autophagy. Autophagy. 2011; 7:689–695. [PubMed: 21460635]
55. Reiner A, Dragatsis I, Zeitlin S, Goldowitz D. Wild-type huntingtin plays a role in brain development and neuronal survival. Molecular neurobiology. 2003; 28:259–276. [PubMed: 14709789]
56. Dragatsis I, Efstratiadis A, Zeitlin S. Mouse mutant embryos lacking huntingtin are rescued from lethality by wild-type extraembryonic tissues. Development. 1998; 125:1529–1539. [PubMed: 9502734]
57. Cheong H, et al. Analysis of a lung defect in autophagy-deficient mouse strains. Autophagy. 2014; 10:45–56. [PubMed: 24275123]
58. Ramesh Babu J, et al. Genetic inactivation of p62 leads to accumulation of hyperphosphorylated tau and neurodegeneration. Journal of neurochemistry. 2008; 106:107–120. [PubMed: 18346206]
59. Babu JR, Geetha T, Wooten MW. Sequestosome 1/p62 shuttles polyubiquitinated tau for proteasomal degradation. Journal of neurochemistry. 2005; 94:192–203. [PubMed: 15953362]
60. Dragatsis I, Levine MS, Zeitlin S. Inactivation of Hdh in the brain and testis results in progressive neurodegeneration and sterility in mice. Nat Genet. 2000; 26:300–306. [PubMed: 11062468]
61. White JK, et al. Huntingtin is required for neurogenesis and is not impaired by the Huntington's disease CAG expansion. Nat Genet. 1997; 17:404–410. [PubMed: 9398841]
62. Kegel KB, et al. Huntingtin expression stimulates endosomal-lysosomal activity, endosome tubulation, and autophagy. J Neurosci. 2000; 20:7268–7278. [PubMed: 11007884]
63. Steffan JS. Does Huntingtin play a role in selective macroautophagy? Cell Cycle. 2010; 9:3401–3413. [PubMed: 20703094]
64. Wong YC, Holzbaur EL. The regulation of autophagosome dynamics by huntingtin and HAP1 is disrupted by expression of mutant huntingtin, leading to defective cargo degradation. J Neurosci. 2014; 34:1293–1305. [PubMed: 24453320]
65. Zheng S, et al. Deletion of the huntingtin polyglutamine stretch enhances neuronal autophagy and longevity in mice. PLoS Genet. 2010; 6:e1000838. [PubMed: 20140187]

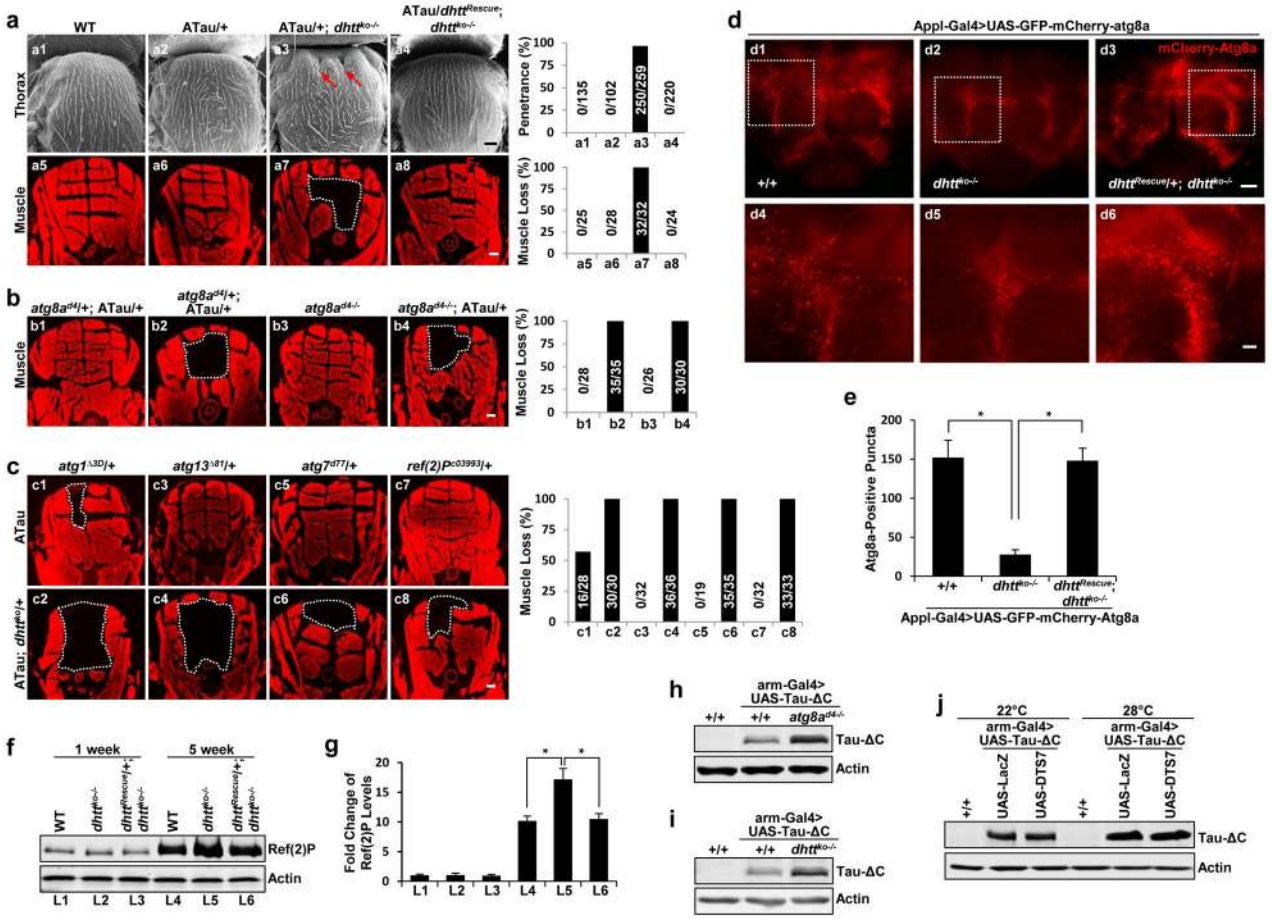

Figure 1. ***Drosophila huntingtin*** **interacts genetically with the autophagy pathway**

(a) Representative Scanning Electron Microscopy (SEM) images of the external thorax (a1–a4) and Phalloidin F-actin staining of the internal muscle structure underlying the thorax (a5–a8) in adult flies of the indicated genotype. Arrows: collapsed thorax. White dashed lines: missing dorsal longitudinal muscles. "ATau": ectopic Tau expression from a single copy of UAS-Tau transgene driven by a single copy of A307-Gal4 line (A307-Gal4>UAS-Tau/+). *Right:* quantification of penetrance (top) or muscle loss (bottom) (n=3 independent experiments).

(b,c) Phalloidin F-actin staining in fly mutants of the indicated genotypes either homozygous for $atg8a^{d4}$ or double heterozygous for $dhtt^{ko}$ and other mutations: $atg8a^{d4}$, $atg1^{\Delta 3D}$, $atg13^{\Delta 81}$, $atg7^{d77}$ and $Ref(2)P^{c03993}$. *Right:* quantification of percentage of muscle loss (n=4 independent experiments).

(d, e) Representative confocal images of whole-mount adult brains expressing mCherry-GFP-Atg8a reporter under a pan-neuronal driver (Appl-Gal4) (d4–d6). High-magnification view of boxed areas. (e) Quantification of the mCherry-Atg8a-positive puncta in the flies of the indicated genotypes. (n=15 fly brains (d1), n=18 (d2), n=19 (d3), pooled from 3 independent experiments).

(f,g) Representative immnoblot (f) and quantification (g) of Ref(2)P protein from *dhtt*$^{ko-/-}$ mutant flies and age-matched controls with the indicated genotypes. (n=3 independent experiments).

(h–i) Representative immunoblot of Tau-ΔC in fly mutants homozygous for *atg8a*^{d4} (h) or *dhtt*^{ko} (i). (j) Representative immunoblot of samples from flies co-expressing Tau-ΔC together with control LacZ (lanes 2 and 5) or with DTS7 (lanes 3 and 6), a temperature-sensitive dominant-negative mutant allele of a proteasome subunit. Inactivation of the proteasome by raising DTS7-expressing flies at non-permissive 28°C (lanes 4–6) did not cause higher level of accumulation of Tau-ΔC compared to control. All values are mean +s.e.m. and differences are significant for *P<0.05 using analysis of variance + Bonferroni test. Scale bars: 20 μm for d4–d6 and 100 μm for all the others. Uncropped images of blots are shown in Supplementary Figure 9.

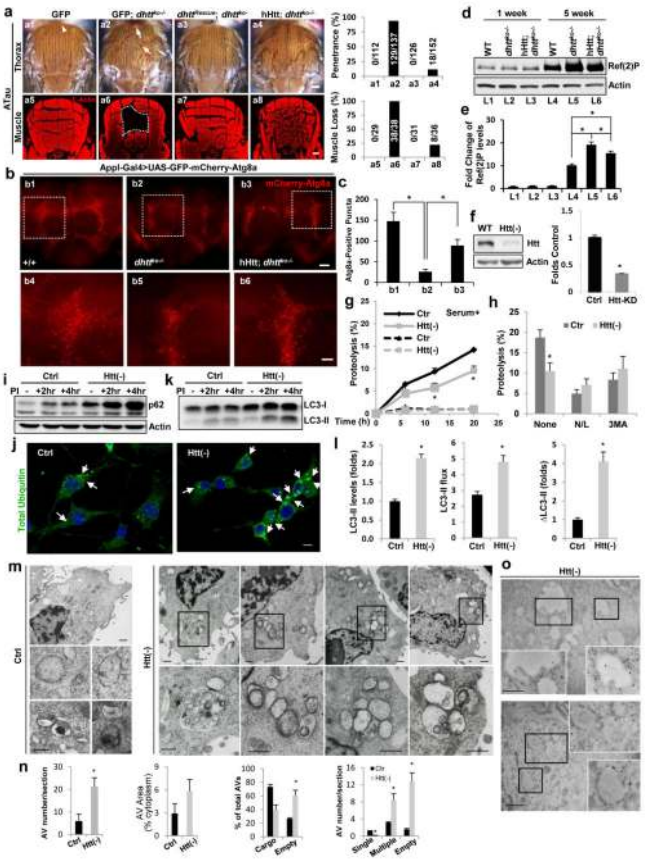

Figure 2. Huntingtin is functionally conserved between the fly and humans and is required for effective autophagy in mammals

(a–e) Human Huntingtin (hHtt) rescued *dhtt*^{ko}-associated phenotypes. **(a)** Thorax pictures (top) and Phalloidin F-Actin staining (bottom) of flies. Arrows: collapsed thorax. White dashed lines: muscle loss. Scale bar: 100 μm Right: quantification. **(b)** Representative confocal images of adult brains from GFP-mCherry-Atg8a expressing flies (scale bar: 100 (top) and 20 (bottom) μm. **(c)** Quantification. n=12 fly brains (b1), n=10 (b2), n=9 (b3), pooled from 3 independent experiments. **(d)** Representative Ref(2)P immunoblot in mutants flies of the indicated ages and genotypes. **(e)** Quantification. (n=3 independent experiments). (**f–o**) Autophagic activity in NIH3T3 mouse fibroblasts control (Ctr; transduced with empty vector) or knockdown for Htt (Htt(−)). (**f**) Immunoblot for Htt and quantification; (n=8). (**g**) Long half-life protein degradation rates (g) in cells cultured in serum-supplemented medium without additions (continuous line) or upon addition of lysosomal proteolysis inhibitors (ammonium chloride and leupeptin (N/L)) (discontinuous line) (n=6 plates in 6 independent experiments (with triplicate wells per condition). (**h**) Effect of N/L or treatment with 3-methyladenine (3MA) to inhibit macroautophagy, (n=6 plates in 6 independent experiments (with triplicate wells per condition). (**i**) Representative immunoblot of p62 in cells untreated (−) or treated for the indicated times with lysosomal protease inhibitors (PI). (**j**) Immunofluorescence for polyubiquitinated proteins. Arrows: protein aggregates. Scale bar: 10μm. (**k,l**) LC3-II flux in cells treated as in (i); representative immunoblot (k) and quantification (l) of LC3-II steady-state levels (left), net flux (middle) and synthesis

(difference between 2 and 4 hr) (right) (n=6 plates in 6 independent experiments (with triplicate wells per condition).; (**m**) Representative electronmicrographs of cells maintained in serum-supplemented media. Bottom: higher magnification images of the boxed areas; (n) Quantification (from left to right) of AV number per section, relative cytosolic area occupied, percentage containing cargo and number per section containing single (selective) or multiple (in bulk) cytosolic content or an empty lumen, (n=12 micrographs for each condition from 3 independent experiments (4 micrographs/experiment)). (**o**) Representative images of immunogold labeling for LC3. Insets: Boxed areas at higher magnification. Scale bars: 2 μm. All values are mean+s.e.m. and differences are significant for *P<0.05 using either analysis of variance + Bonferroni test (e,c) or student's t-test (f,h,l,n) Uncropped images of blots are shown in Supplementary Figure 9.

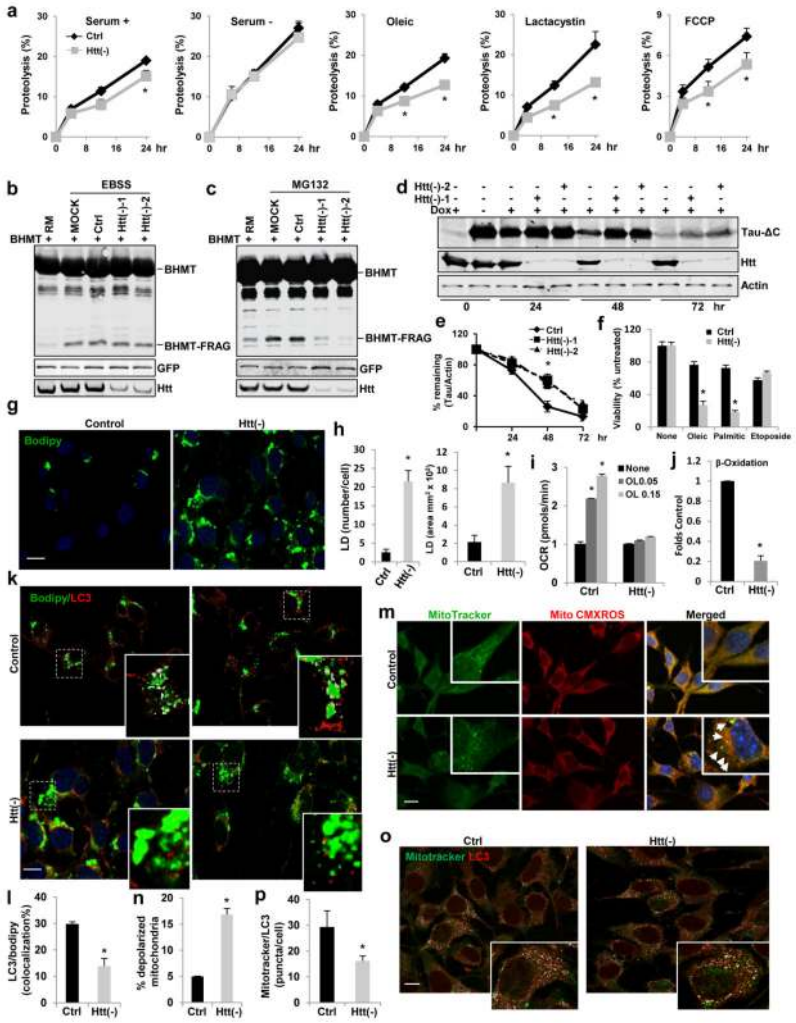

Figure 3. Huntingtin functions in selective macroautophagy

(a) Htt loss reduced autophagy-dependent degradation in response to different stressors. Long half-life protein degradation rates in NIH3T3 cells control (Ctr) or knockdown for Htt (Htt(−)) cultured in serum deprived (−) or supplemented (+) medium without additions or with the indicated stressors. (n=6 plates in 3 independent experiments (with triplicate wells per condition)).

(b,c) GST-BHMT assay. Representative immunoblot for GST-BHMT in HEK293T cells treated as indicated (n=3 independent experiments). **(d,e)** Tau-ΔC degradation. Representative immunoblot of the time-course of Tau-ΔC levels in HeLa cells (d) and quantification of Tau-ΔC protein (e) (n=3 independent experiments).

(**f–l**) Htt knockdown in NIH3T3 fibroblasts reduces lipophagy. (f) Higher susceptibility of Htt(−) cells to lipotoxicity (oleic or palmitic acid) but not to genotoxicity (etoposide),) (n=6 plates in 3 independent experiments (with triplicate wells per condition).. (g,h) Accumulation of lipid droplets (LD) in oleic-treated cells. Representative images of Bodipy493/503-stained cells (g) and quantification of LD number per cell and average LD area (h). Scale bar: 10 μm. (n=3 independent experiments where a total of 100 cells were analyzed per condition). (i) Reduced increase in oxygen consumption rates (OCR) upon

oleic (O) challenges,) (n=6 plates in 4 independent experiments (with 4 wells per condition). (j) Reduced beta-oxidation measured as release of [^{14}C]-carbon dioxide in [^{14}C]-oleate-loaded cells, (n=4). (k,l) LC3 immunostaining in BODIPY493/503-stained cells. (k) Representative images (insets: higher magnification of boxed areas with colocalization pixels in white). Scale bar: 10 μm. (l) Quantification: percentage of LC3/BODIPY colocalization. (n=3 independent experiments a total of 110 cells were analyzed per condition).

(**m–p**) Htt knockdown in NIH3T3 fibroblasts reduces mitophagy. (m,n) Htt(−) cells have higher content of depolarized mitochondria (MitoTracker-positive and MitoTracker-Red-CMXROS-negative). (m) Representative images (insets: higher magnification images). Arrows: depolarized mitochondria. Scale bar: 10 μm. (n) Quantification: percentage of depolarized mitochondria. (n=3 independent experiments a total of 85 cells were analyzed per condition). (**o,p**) LC3 immunostaining in MitoTracker-stained cells. (o) Representative images in both channels and colocalization pixels in white (insets: higher magnification images). Scale bar: 10 μm. (p) Quantification of LC3/MitoTracker colocalization. (n=3 independent experiments where a total of 110 cells were analyzed per condition). In all studies with lentivirus-mediated shRNA (f–p) control cells were transduced with viral particles carrying the empty vector.

All values are mean+s.e.m. and differences are significant for *P<0.05 using student's t-test (a,f–p) or analysis of variance + Bonferroni test (e). Uncropped images of blots are shown in Supplementary Figure 9.

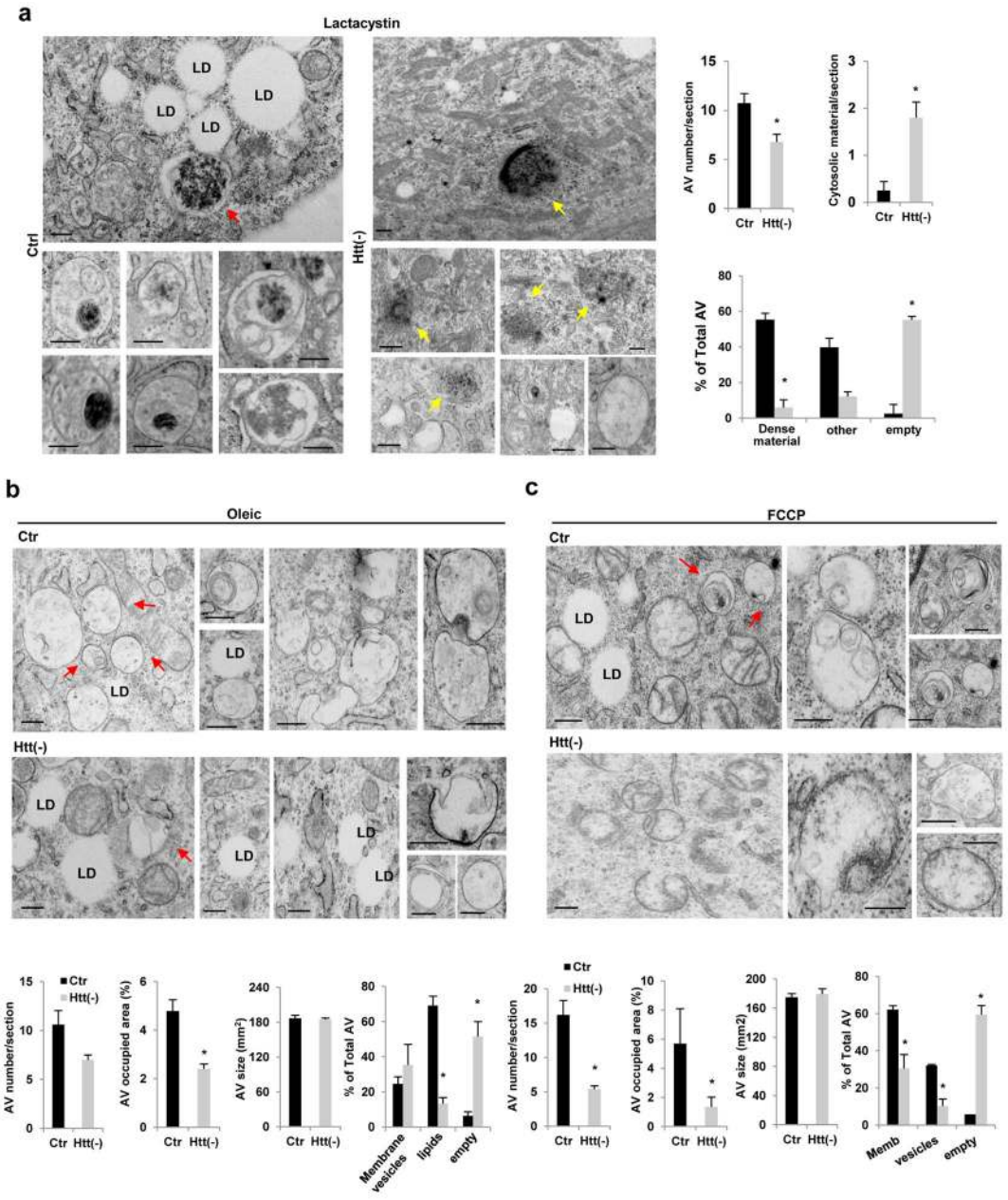

Figure 4. Ultrastructure of cells knockdown for Huntingtin upon induction of selective types of autophagy

NIH3T3 fibroblasts control (Ctr) or knockdown for Htt (Htt(−)) were exposed to lactacystin (**a**), oleic acid (**b**) or mitochondria depolarizing agent FCCP (**c**) and processed for electron microscopy. Images show representative cellular areas and insets show examples of autophagic vacuoles (AV) at higher magnification to appreciate cargo content. Red arrows: protein aggregates inside AV (a), AV containing lipid material (b) or AV containing mitochondria (c). Yellow arrows: protein aggregates free in the cytoplasm. LD: lipid droplets. Note that induction of proteotoxicity with lactacystin favors autophagic sequestration of proteinaceous aggregate material over sequestration of LD that remain

intact under these conditions (a), whereas induction of lipophagy with oleic, results in higher content of AV in close proximity of the LD (b). LD are also preserved from autophagic sequestration in the case of FCCP treatment, where membranous structures compatible with mitochondria undergoing degradation are detected in AV (c). Quantification of the number, average size and percentage of cytosolic area covered by AV is shown on the right (a) or at the bottom (b,c). (n=9 (in a), 9 (in b) ad 6 (in c) micrographs pooled from 3 independent experiments). Scale bars: 0.5 μm. All values are mean+s.e.m. and differences are significant for *P<0.05 using student's t-test.

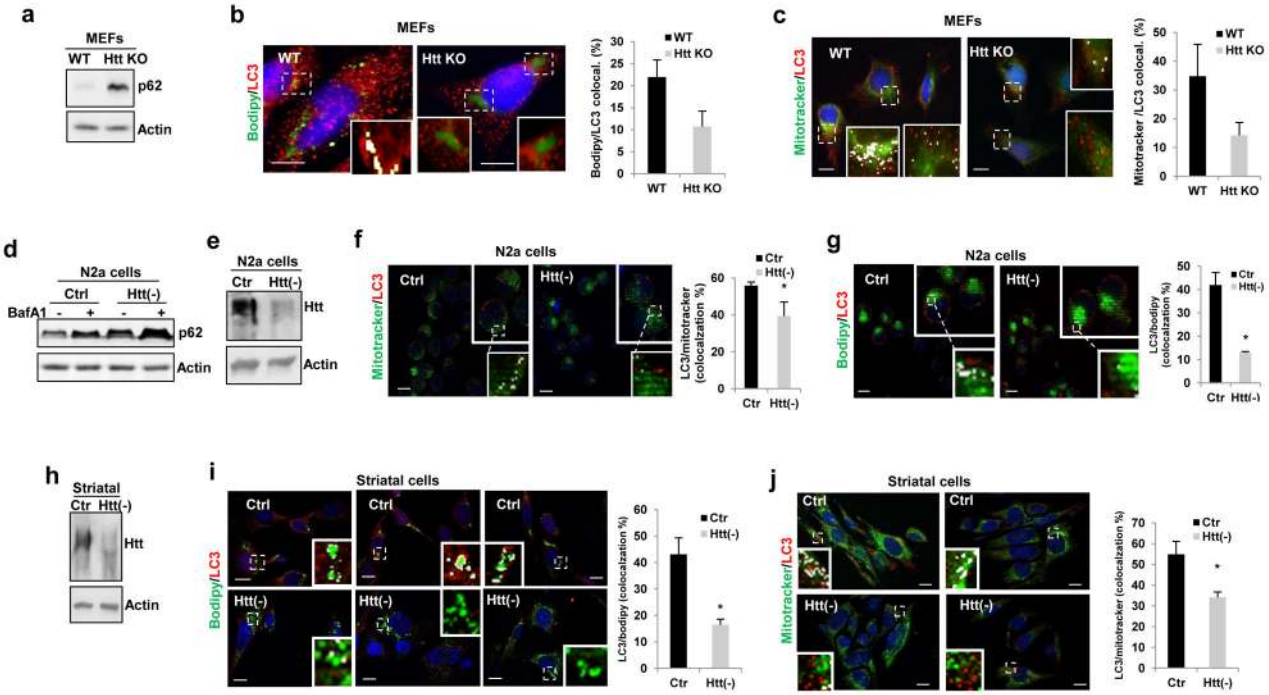

Figure 5. Role of Huntingtin in selective autophagy in different mammalian cell types

Defective selective autophagy in different types of mammalian cells with reduced Htt levels. (a,d) Representative immunoblots to illustrate increased levels of p62 in total cellular lysates of mouse embryonic fibroblasts (MEFs) from mouse knock-out for Htt (HttKO) (a) or N2a cells knockdown (KD) for Htt (Htt(−)) untreated (−) or treated with BafA1 (d). Analysis of lipophagy and mitophagy as the colocalization of LC3 with BODIPY493/503-stained lipid droplets (b,g,i) or with MitoTracker®-labeled mitochondria (c,f,j) in MEFs from wildtype (WT) or Htt-KO mice (b,c), in N2a neuroblastoma cells (f,g) and mouse striatal derived cells (i,j) control or knocked-down for Htt (Htt(−)) upon exposure to oleic acid (for lipophagy) or FCCP (for mitophagy). Efficiency of knockdown was confirmed by immunoblot (e,h). Quantification of the percentage of colocalization in shown at the right. Images show merged channels and inserts show colocalization mask (as white pixels). Scale bars: 10 μm. The number of independent experiments (n) was 3 (in b, c,i,j) and 4 (in f,g) where the number of total cells counted for each experimental condition were 80 (b), 75 (c), 80 (f), 60(g), 80 (i) and 70 (j). All values are mean+s.e.m. and differences are significant for *P<0.05 using student's t-test.

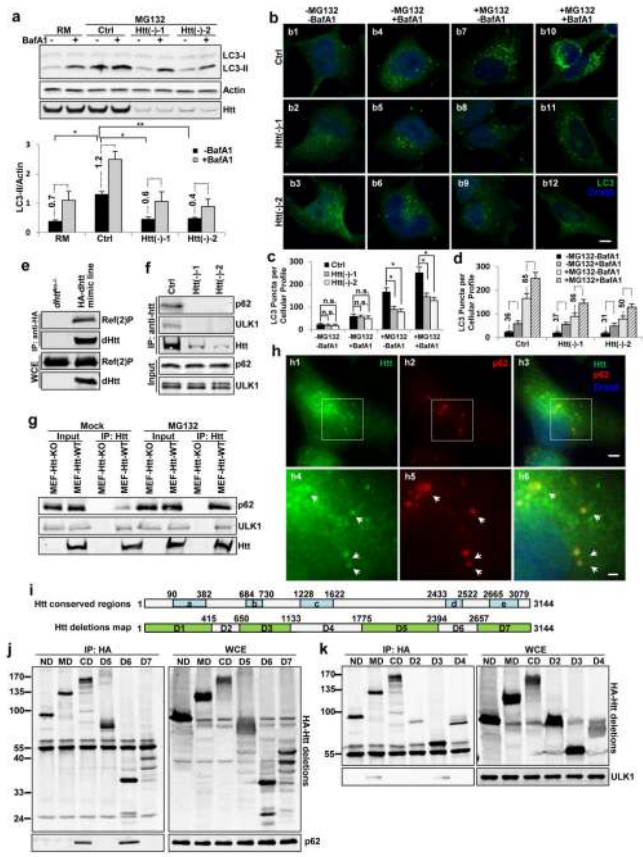

Figure 6. Huntingtin modulates autophagic induction and physically interacts with p62 and ULK1 proteins through two non-overlapping conserved regions

(**a**) Representative immunoblot for LC3 in HEK293T cells treated as indicated. Bottom: quantification of LC3-II levels and net LC3-II flux (lateral numbers shown net differences in LC3-II levels upon addition of BafA1) normalized against loading control actin. (n=3 independent experiments) (**b**) Immunostaining for LC3 in HeLa cells treated as indicated. (**c–d**) Quantification of LC3-positive puncta plotted by different inhibitor treatments (c) or by Htt genotype (d). Note that although the ratio of LC3 in cells treated or not with BafA1 is comparable in control and Htt(−) cells, the net changes in LC3 puncta content upon addition of BafA1 (shown in the lateral numbers) are markedly lower in these cells (n=5 wells, pooled from pooled from 3 independent experiments, >150 cells per experiment). Scale bar: 10 μm.

(e) Representative immunoblot to show co-immunoprecipitation (co-IP) experiments using whole-animal extract from *dhtt*$^{ko-/-}$ as negative control or a genome-tagging MiMIC fly line expressing 3XHA-tagged dHtt. (n=3 independent experiments).

(f,g). Representative immunoblot to show co-IP experiments between Htt and p62 or ULK1 in HEK293T cells (f) and MEF cells (g) in comparison with negative controls si-Htt-treated (f) or MEF-Htt-KO (g) cells. Input lines show the Triton X100-soluble fraction from the whole cell lysate used for co-IP upon normalization of soluble p62 levels across samples. (n=3 independent experiments).

(h) Representative confocal images of immunofluorescent stained cells for Htt (green), p62 (red) and Draq5 (blue). Bottom: high-magnification view of boxed areas. Scale bar: 5 μm (top) or 2 μm (bottom) (n=3 independent experiments).

(i–k) Mapping of p62 and ULK1-interacting regions in Htt. (i) Schematics of fly and human conserved regions (blue) in Htt (top) and of the Htt deteltions (green) generated in this study (bottom). (j,k) Representative immunoblots for co-IP assays using the HA-tagged Htt deletions to pulldown Myc-p62 (j) or Myc-ULK1 (k). Whole cell extracts (WCE) are shown in the right. Myc-p62 was pulled down by the C-terminal CD and D6 fragments in Htt and Myc-ULK1 by the middle MD and D3 fragments in Htt. All values are mean+s.e.m. and differences are significant for *P<0.05 using analysis of variance + Bonferroni test. Uncropped images of blots are shown in Supplementary Figure 9.

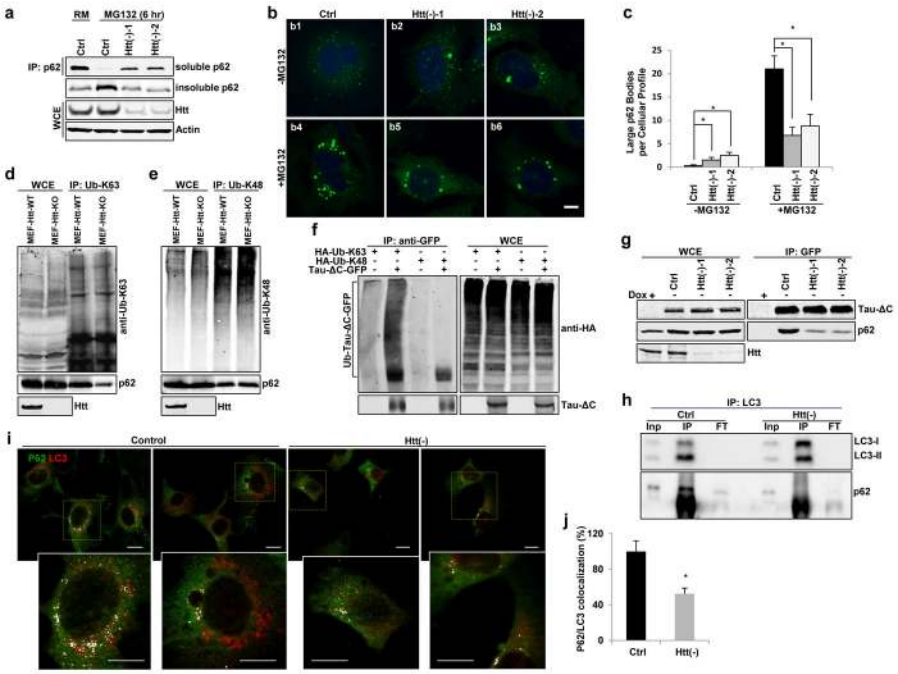

Figure 7. Huntingtin facilitates p62-mediated cargo recognition efficiency

(a) Representative immunoblot of Triton X-100 soluble and insoluble p62 in HEK293T cells treated as indicated (n=3 independent experiments).

(b) Confocal images of HeLa cells immunostained for endogenous p62 (green) and Draq5 (blue). Scale bar: 8 μm. (c) Quantification of large p62 bodies. n=3 independent experiments>150 cells

(d–e) Representative immunoblots of endogenous proteins with Ub-K63 or Ub-K48 modifications immunoprecipitated in MEFs cells from wildtype (WT) or Htt knock-out (Htt-KO) mice using anti-Ub-K63 (d) or anti-Ub-K48 (e) antibodies. Co-immunoprecipiated p62 is also shown. (f) Tau-ΔC-GFP and HA-tagged Ub-K63 or Ub-K48 were co-transfected into HEK293T cells, followed by in vitro ubiquitination assay with anti-GFP antibody and probed with anti-HA antibody. (g) Representative immunoblots of endogenous p62 co-immunoprecipitated with an anti-GFP antibody in stable Tau-ΔC-GFP expressing HeLa cells control or treated with siRNA against Htt (n=3 independent experiments).

(**h–j**) Htt knockdown compromised p62/LC3 interaction in NIH3T3 fibroblasts. (h) Representative immunoblot of Co-IP experiments in NIH3T3 cells for LC3. Inp: input, IP: immunoprecipitated, FT: flow-through. (i,j) Co-immunostaining for p62 and LC3 in confluent NIH3T3 cells. (i) Representative images of merged channels of full fields (top) and high magnification of boxed areas (bottom). Scale bar: 10 μm. (j) Quantification: percentage of colocalization. (n=4 independent experiments a total of 80 cells were analyzed per condition). All values are mean+ s.e.m. and differences are significant for *P<0.05 using analysis of either variance + Bonferroni test (c) or student's test (j). Uncropped images of blots are shown in Supplementary Figure 9.

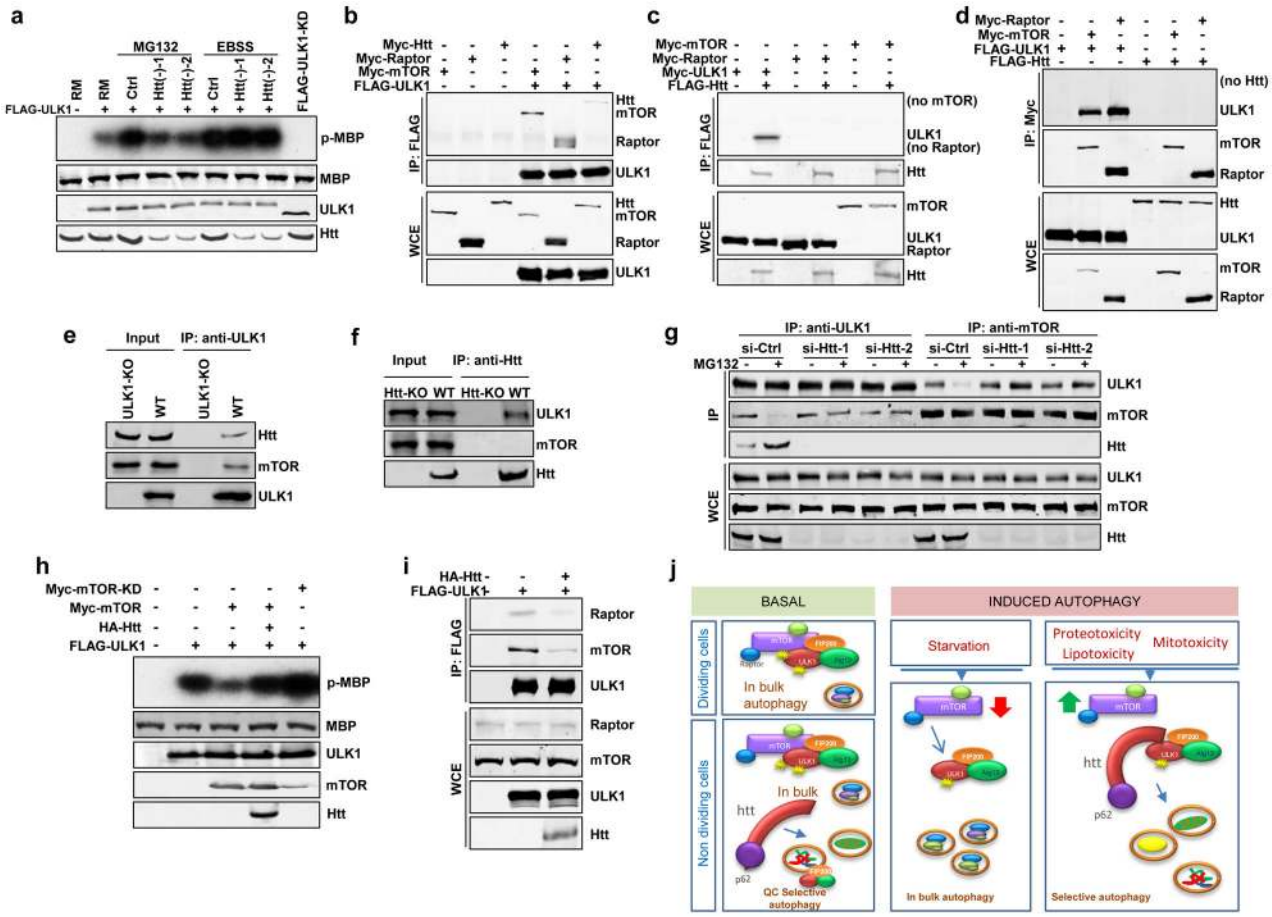

Figure 8. Huntingtin-ULK1 and mTOR-ULK1 complexes are mutually exclusive

(a) Representative autoradiograph to show *in vitro* ULK1 kinase activity monitored by the phosophorylation level of myelin binding protein (p-MBP). Equal input of ULK1 protein was verified by immunoblot. (n=3 independent experiments).

(b) Representative immunoblot of co-immunoprecipitation (co-IP) experiments using anti-FLAG antibody in HEK293T cells co-transfected with FLAG-tagged ULK1 and Myc-tagged Htt, Raptor, or mTOR, as indicated (n=3 independent experiments).

(c, **d)** Representative immunoblot of Co-IP experiments using anti-FLAG (c) or anti-Myc (d) in in HEK293T cells co-transfected with tagged Htt, ULK1, mTOR and Raptor, as indicated. **(e**, **f)** Representative immunoblots of endogenous co-IP experiments in MEFs using anti-ULK1 (e) or anti-Htt antibodies (f). **(g)**. Representative immunoblot to show reciprocal co-IP experiments in MEFs using anti-ULK1 or anti-mTOR antibodies, as indicated. **(h)** Representative immunoblot to show *in vitro* ULK1 kinase assay in HEK293T cells treated as indicated **(i)** Representative immunoblot of co-IP assays using anti-FLAG in HEK293T cells transfected with FLAG-ULK1 and HA-Htt as indicated to analyze association between ULK1 and endogenous Raptor or mTOR proteins (n=3 independent experiments).

(j) A schematic model of Htt regulation of selective autophagy. Htt serves as scaffolding for selective autophagy by bringing together cargo bound through p62 and the initiator of autophagy ULK1. Basal autophagy: under basal conditions the absence of Htt leads to

reduced selectivity in cargo recognition required for quality control autophagy, but it does not affect autophagy induction/autophagosome biogenesis, since basal ULK1 is sufficient to sustain “in bulk” autophagy and basal quality control autophagy. Induced autophagy: maximal activation of autophagy in response to stress requires the release of mTORC1 inhibition over ULK1. In starvation-induced autophagy inactivation of mTORC1 promotes release and activation of ULK1. Selective autophagy induced in response of different stressors requires Htt to actively compete away ULK1 from the mTORC1 inhibitory complex.